JACS
JOURNAL OF THE AMERICAN CHEMICAL SOCIETY

COMMUNICATION

pubs.acs.org/JACS

Combinatorial Discovery of Fluorescent Pharmacophores by Multicomponent Reactions in Droplet Arrays

Olga N. Burchak,[†] Laurent Mugherli,[†] Mariano Ostuni,[‡] Jean Jacques Lacapère,[‡] and Maxim Y. Balakirev*[,†]

[†]Biomics Laboratory, Institut de Recherches en Technologies et Sciences pour le Vivant, CEA, 17 rue des Martyrs, 38054 Grenoble, France

[‡]Unité INSERM U773, Centre de Recherche Biomédicale Bichat Beaujon CRB3, Université Paris 7 Denis Diderot, BP 416, F-75018 Paris, France

Supporting Information

ABSTRACT: Fluorescence imaging in clinical diagnostics and biomedical research relies to a great extent on the use of small organic fluorescent probes. Because of the difficulty of combining fluorescent and molecular-recognition properties, the development of such probes has been severely restricted to a number of well-known fluorescent scaffolds. Here we demonstrate that autofluorescing druglike molecules are a valuable source of bioimaging probes. Combinatorial synthesis and screening of chemical libraries in droplet microarrays allowed the identification of new types of fluorophores. Their concise and clean assembly by a multicomponent reaction presents a unique potential for the one-step synthesis of thousands of structurally diverse fluorescent molecules. Because they are based upon a druglike scaffold, these fluorophores retain their molecular recognition potential and can be used to design specific imaging probes.

Fluorescent labeling of biologically active molecules is widely employed to study their functions within cells and whole organisms.[1] In drug discovery and chemical genetics, fluorescent tagging of a pharmacophore allows its intracellular visualization and identification of its potential targets. Even though fluorescent labels are relatively small, their incorporation can change the properties of the pharmacophore, thereby limiting their application. The ideal pharmacophore should display its own specific fluorescent signature to allow "label-free" visualization. Such a marriage of molecular-recognition and fluorescent properties within one molecule would create a valuable source of imaging probes for biomarker discovery. One way to achieve this goal is to explore the chemical space around the known fluorophore cores to search for fluorescent druglike molecules with specific recognition properties.[2] This approach is illustrated in the diversity-oriented fluorescence libraries developed by Chang and coworkers,[2] which have been successfully used to create fluorescent probes for various biological targets. Although combinatorial synthesis based on a known fluorophore core avoids the synthetic challenge of discovering fluorophores de novo, it also limits the structural diversity of the chemical library to specific fluorescent scaffolds that do not necessarily have druglike properties. Another approach is to transform the druglike scaffolds into fluorescent molecules. In fact, many natural and synthetic pharmacophores exhibit intrinsic fluorescence that is often neglected or considered an undesirable "false positive" in drug screening.[1,3] Such molecules could serve as starting points for combinatorial searches for new fluorescent scaffolds.

Imidazo[1,2-*a*]pyridines are naturally occurring synthetic compounds that are widely used in medicinal chemistry. In our screens for inhibitors of the NS3/4A serine protease of the hepatitis C virus,[4] some of the imidazo[1,2-*a*]pyridines autofluoresced in UV and interfered with the enzymatic assay. Because imidazo[1,2-*a*]pyridine-related heterocycles can be produced by the three-component Ugi reaction (3-CR) of aromatic amidines with aldehydes and isocyanides,[5] we screened a panel of 3-CRs to determine whether some would yield fluorophores with fluorescence in the visible region. One advantage of MCRs is the relative ease of their parallelization, which allows an array of reactions to be performed in a microplate or on a planar solid support.[6] We set up 3-CRs in 100 nL droplets aligned on a glass slide with a surface-tension microarray.[4] Each microarray had 800 hydrophilic spots patterned on a hydrophobic surface to maintain the positions of the droplets.[4] In parallel, we found that volatile isocyanides could be added to the arrayed aminopyridine−aldehyde mixtures via adsorption from the gas phase, which avoided the need to dispense these malodorous, potentially toxic compounds. Five 3-CRs were examined to validate synthesis on the patterned support [Figure S1 in the Supporting Information (SI)]. Each reaction was conducted on an individual slide with 100 nL droplets of 1:1 dimethyl sulfoxide (DMSO)/water containing an aminopyridine−aldehyde mixture (each 2 mM) and scandium triflate as the Lewis acid catalyst (5% mol). The array was placed in a hermetic chamber saturated with isocyanide vapor; afterward, the droplets were combined and analyzed by high-performance liquid chromatography (HPLC) and electrospray ionization mass spectrometry (ESI-MS). At 20 h, the yield of aminoimidazo[1,2-*a*]pyridines was generally sufficient (>10%) to detect the formation of fluorescent compounds (Figure S1).

To discover new fluorophores, eight heterocyclic amidines (A1−A8), 40 aldehydes (B1−B40), and five isocyanides (C1−C5) were mixed in arrayed droplets to provide 1600 unique combinations (Figure 1a and Figure S2a). Each glass slide contained 8 × 40 = 320 aminopyridine−aldehyde mixtures spotted in duplicate. The slides were then exposed to an isocyanide, and the fluorescence was analyzed with a microarray scanner at four different filter settings (Figure 1b and Figure S2b).

Received: May 2, 2011
Published: June 06, 2011

dx.doi.org/10.1021/ja204016e | *J. Am. Chem. Soc.* 2011, 133, 10058–10061

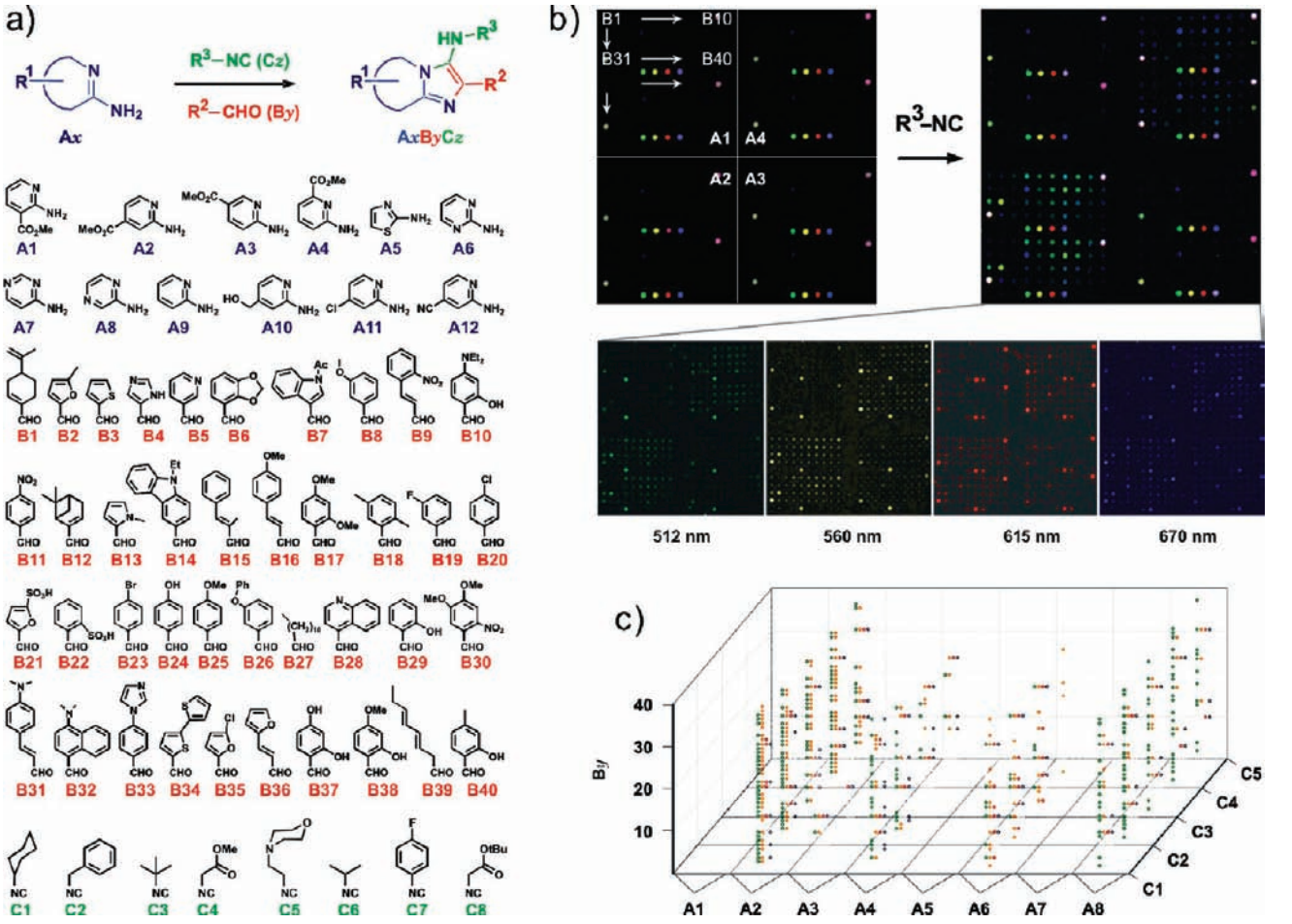

Figure 1. Combinatorial screening of fluorophores with a surface-tension microarray. (a) Synthesis of the chemical library by the three-component Ugi reaction (3-CR). (b) Representative fluorescent scanner images of the 3-CR screen showing the reactions of A1−A4, the four positional isomers of carboxymethyl-2-aminopyridine, with the 40 aldehydes B1−B40 and cyclohexyl isocyanide (C1). Microarray fluorescence (right) with and (left) without exposure to isocyanide vapor is shown. Each picture is a merge of four false-color images taken at different wavelength settings (lower panel). The repeated four-color spot motif is a set of control fluorophores: fluorescein, Cy3, TxR, and Cy5. (c) Cumulative microarray 3-CR profiling results for eight amidines A*x*, 40 aldehydes B*y*, and five isocyanides C*z*. Each point corresponds to the formation of a fluorescent compound in the reaction A*x* + B*y* + C*z* recorded at a given wavelength (coded by the corresponding colors).

The fluorescence of each droplet was compared with that of a control microarray incubated without isocyanide. We observed that exposure of the slides to isocyanide resulted in the appearance of a distinctive pattern of fluorescent spots (Figure 1b and Figure S2b). The microarray thus functions as a kind of "chemical nose" that reports the presence of the volatile isocyanide by its fluorescence signal. Analysis of the microarray data revealed the crucial role of the amidine structure in the appearance of fluorescence. The four amidines A2, A4, A6, and A8 gave rise to fluorescent signals, with A2 and A8 being the most efficient (Figure 1c and Figure S2b). Aminopyridine A2 produced mainly yellow and green spots, while aminopyrazine A8 yielded predominantly green spots. Both A4 and A6 produced fewer and weaker fluorescent signals with apparently red-shifted emissions. With the same aminopyridine, the color of the 3-CR changed significantly depending on the aldehyde structure, while the isocyanide component did not have a major effect on the fluorescence pattern. Other amidines did not produce visible fluorophores except when reacted with the inherently fluorogenic aldehydes B10, B14, and B31 (Figure 1c).

The amidines A2, A4, A6, and A8 identified by microarray screening were then used in scaled-up 3-CRs to synthesize a small library of ~60 compounds. We named these compounds "Flugis", which stands for *Flu*orescent *Ugi* products. In addition, amidines A8−A12 and isocyanides C6−C8 were introduced to investigate more extensively the structure−fluorescence relationship of Flugis (Figure 2). We found that all four fluorogenic amidines exhibited an intrinsic fluorescence in the UVA region, albeit with different efficiencies (A2, A4, A6, and A8 in Figure 2). For amidines A2 and A8, the formation of the Flugi framework was accompanied by a large (up to ~150 nm) bathochromic shift in the fluorescence of the compound (Figure 2 and Figure S3a). The amino group at position 3 was required for the observed red shift because the corresponding unsubstituted compounds had fluorescence similar to the initial amidines (compare compounds A2, Flugi_**0**, and Flugi_**1** in the table in Figure 2; for spectra, see Figure S3a). The bathochromic effect was even more pronounced in the case of Flugis derived from amidines A4 and A6 (Flugi_**3** and Flugi_**4**), resulting in exceptionally large fluorescence Stokes shifts (Figure 2). For Flugi_**3**, the Stokes shift reached 272 nm (12 220 cm^{-1}), which is one of the largest

dx.doi.org/10.1021/ja204016e |*J. Am. Chem. Soc.* 2011, 133, 10058–10061

Flugi #	Structure	λ_{abs}[a] [nm]	λ_{em}[a] [nm]	ϕ_f[b]
	A2	342	424	0.28
	A4	326	411	0.27
	A6	296	350	0.005
	A8	321	382	0.40
0[c]	A2B25-**H**	355	427	0.39
1[d]	A2B25-**NH_2**	426	520	0.43
2	A2B25C1	387	528	0.49
3	A4B25C1	355	627	0.002
4	A6B25C1	365	560	0.009
5	A8B25C1	355	491	0.46
6	A9B25C1	350	490	0.25
7	A10B25C1	341	495	0.29
8	A11B25C1	357	518	0.08
9	A12B25C1	389	525	0.42
10	A2B27C1	368	516	0.24
11	A8B27C1	329	485	0.21
12	A2B23C1	388	524	0.42
13	A2B8C1	384	526	0.51
14	A2B33C1	387	529	0.83
15	A2B13C1	392	530	0.64
16	A2B38C1	391	531	0.10
17	A2B35C1	392	532	0.67
18	A2B4C1	400	532	0.63
19	A2B21C1	393	533	0.31
20	A2B37C1	394	534	0.10
21	A2B2C1	398	535	0.71
22[e]	A2B2C1^{Me+I-}	399	568	0.42
23	A8B2C1	368	500	0.46
24	A2B22C1	382	539	0.62
25	A2B15C1	392	542	0.51
26	A2B36C1	413	558	0.37
27	A2B16C1	414	559	0.42
28	A8B16C1	365	514	0.23
29	A2B31C1	434	573	0.35
30	A8B31C1	407	520	0.24
31	A2B16C7	400	528	0.27
32	A2B16C5	384	542	0.52
33	A2B16C3	416	554	0.48
34	A2B16C8	410	555	0.37
35	A2B16C4	411	556	0.39
36	A2B16C2	419	556	0.52
37	A2B16C6	413	558	0.49

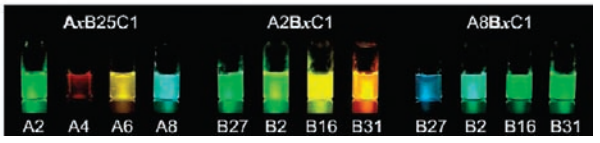

Figure 2. Fluorescence properties of Flugis. The table at the top shows absorption and emission maxima of selected fluorophores. The panel at the bottom shows the fluorescence of representative Flugis in DMSO solution as visualized with a 365 nm UV lamp. The concentrations of the fluorophores were 1 μM, except for those of A4B25C1 (Flugi_**3**) and A6B25C1 (Flugi_**4**), which were 100 μM. Notes: [a]Absorption and fluorescence emission spectra were recorded in DMSO. [b]Quantum yields were measured using fluorescein ($\varphi_f = 0.92$) and 2-aminopyridine ($\varphi_f = 0.60$) as external standards. [c]A2B25−H was synthesized by the condensation of 2-aminopyridine (A2) with 4-methoxyphenacyl bromide. [d]A2B25−NH_2 was synthesized by Pd-catalyzed hydrogenolysis of A2B25C2. [e]A2B2C1^{Me+I-} was synthesized by alkylation of A2B2C1 in neat methyl iodide. (For experimental procedures regarding notes [c], [d], and [e], see the SI).

values reported for a small organic fluorophore. However, these compounds were significantly less bright than the Flugis derived from A2 and A8 and less useful as imaging probes (Figure 2 and Figure S3). The Flugis derived from amidines A2 and A8 had extinction coefficients (ε) in the range $(1.1-2.7) \times 10^4$ M^{-1} cm^{-1} and quantum yields from 0.2 to 0.9, resulting in fluorophore brightnesses B of $\sim 10^4$ M^{-1} cm^{-1}, which is comparable to that of many commercial fluorescent dyes.[1] Consequently, we focused our analysis on the Flugis derived from aminopyridine A2, which exhibited fluorescence in the visible spectrum with a high quantum yield.

Replacing the carboxymethyl residue at the 7-position with other substituents influenced both the absorption spectra and the fluorescence emission spectra of the Flugis (Figure 2 and Figure S4). We observed an almost linear correlation between the spectral maxima and the Hammett substituent constant (σ_p); both the absorption maximum and fluorescence emission maximum shifted to longer wavelengths as the electron-withdrawing ability of the substituent increased (Figure S4). It is plausible that the Flugi fluorescence depends on internal charge transfer (ICT)[7] from the 3-amino group to the heterocyclic framework. Indeed, blocking the electron-donating ability of the nitrogen by acylation or replacement of the amino group with a nitroso residue abolished the fluorescence (not shown), while introduction of an electron-withdrawing *p*-fluorophenyl residue induced a hypsochromic shift of ~30 nm (Figure 2, Flugi_**27** vs Flugi_**31**). The presence of an ICT state is also supported by the almost structureless emission spectra and the solvatochromism of the Flugi fluorescence (Figure S5). The spectral and chemical properties of Flugis could be tuned further by varying the aldehyde-derived substituent at the 2-position. The fluorescence color changed from blue to red according to the increasing potential for electron donation and the degree of conjugation of this residue (Figure 2, Flugi_**10**−**29**). The Flugis derived from aminopyrazine A8 showed a similar trend, with the fluorescence shifted toward the blue region (Figure 2, Flugi_**11**, _**23**, _**28**, and _**30**). All of the fluorophores exhibited good quantum yields and large Stokes shifts (up to 158 nm). Moreover, methylation of the N1 nitrogen red-shifted the Flugi fluorescence by an additional ~30 nm and further increased the Stokes shift to ~169 nm (Figure 2, Flugi_**21** vs Flugi_**22**). Finally, the isocyanide-derived substituent of the 3-amino group also had some effect on the Flugi fluorescence (Figure 2, Flugi_**31**−**37**). These data show that Flugis represent a new type of fluorophore with a wide color coverage and, as a result of the 3-CR, excellent potential for combinatorial diversification. Fluorescence sensitivity toward substituents and the polarity of the environment make Flugis a promising scaffold for the synthesis of fluorescent probes, sensors, and enzyme substrates.

To demonstrate the potential of Flugis as imaging probes, we aimed to develop a fluorescent ligand for one of the recognized drug targets of imidazo[1,2-*a*]pyridines. Zolpidem and its analogues in the imidazo[1,2-*a*]pyridine family are well-known anxiolitic and sedative medications (Figure S6). These drugs interact with $GABA_A$ benzodiazepine receptors as well as with the peripheral benzodiazepine receptor, now known as the translocator protein (TSPO).[8] The structural determinants for this interaction have been extensively studied.[9,10] In addition to an aromatic residue at the 2-position of the heterocycle, the presence of a carboxamide group at the 3-position seems to be required for biological activity. In alpidem and zolpidem drugs, this group is separated from the imidazo[1,2-*a*]pyridine heterocycle by one methylene residue. Ligands with a two-atom spacer between the heterocycle and the carboxamide residue can still bind to benzodiazepine receptors, albeit with lower affinity.[10] We therefore synthesized a panel of extended zolpidem analogues by 3-CR with *tert*-butyl isocyanoacetate (Figure 3a). To determine whether these compounds could be used as imaging probes for the mitochondrial benzodiazepine receptor TSPO, we studied their localization in PC-3 prostate carcinoma cells. These cells show a high level of TSPO expression that is thought to be a hallmark of prostate cancer.[11] The Flugis were incubated with live cells growing in glass bottom chambers, and their subcellular distributions were determined with an inverted fluorescence microscope using fluorescein filters set at the 60× oil immersion objective. In parallel, mitochondria were visualized with MitoTracker dye. All of the Flugis stained PC3 cells, but the localization of Flugi_**42** most closely matched the mitochondrial distribution pattern (Figure 3b and Figure S7). The Flugi_**43** lacking the disubstituted carboxamide group did not stain mitochondria, demonstrating a preferential localization to the cytoplasm and the

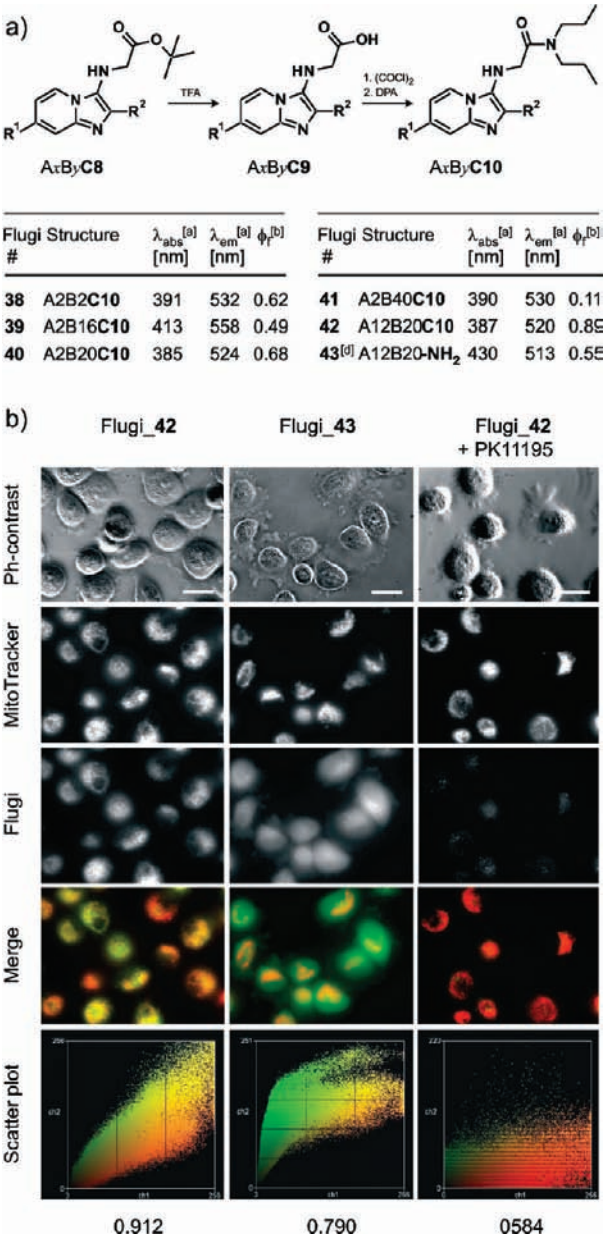

Flugi #	Structure	λ_{abs}[a] [nm]	λ_{em}[a] [nm]	ϕ_f[b]
38	A2B2C10	391	532	0.62
39	A2B16C10	413	558	0.49
40	A2B20C10	385	524	0.68
41	A2B40C10	390	530	0.11
42	A12B20C10	387	520	0.89
43[d]	A12B20-NH_2	430	513	0.55

Figure 3. Synthesis and characterization of fluorescent analogues of zolpidem. (a) Two-step synthesis of zolpidem analogues from A*x*B*y*C10 Flugis. Spectral properties of the synthesized fluorophores are shown in the table. (For notes [a], [b], and [d], see the Figure 2 caption). (b) Fluorescent staining of live PC-3 cells with Flugis. The first column shows colocalization of Flugi_**42** (visualized in the FITC channel) and mitochondria (labeled with MitoTracker Deep Red, Cy5 channel). The colocalization scatter plot with a corresponding Pearson's coefficient of 0.912 is shown at the bottom. The second column shows the different patterns of cell staining observed with Flugi_**43**. The third column shows how Flugi_**42** fluorescent staining was affected by cell preincubation with 25 μM PK11195. Scale bar: 20 μm. For a zoomed view, see Figure S7.

plasma membrane. To determine whether mitochondrial staining by Flugi_**42** was due to its interaction with the benzodiazepine receptor, cells were preincubated with PK11195, a highly specific TSPO ligand. At 25 μM, this compound induced a significant displacement of fluorescent staining, suggesting that Flugi_**42** is a ligand of TSPO (Figure 3b). To characterize this interaction further, the affinities of Flugi_**38**−**43** for TSPO were determined by competition experiments against [3H]PK11195 performed on rat stomach mitochondrial membranes (Figure S8). In these tests, two Flugis had measurable micromolar affinities, and the potency of Flugi_**42** was comparable to that of zolpidem.

In summary, we have demonstrated that autofluorescing drug-like molecules can be a valuable source of bioimaging probes. Combinatorial screening in droplet arrays allowed the de novo discovery of Flugi dyes. We demonstrated fluorescent ligands for benzodiazepine receptors, but other applications of Flugis may be envisaged, such as the development of fluorescent mimics for tryptophan and nucleotides as well as for related drugs.

■ ASSOCIATED CONTENT

Supporting Information. Figures S1−S8, experimental procedures, and compound characterization. This material is available free of charge via the Internet at http://pubs.acs.org.

■ AUTHOR INFORMATION

Corresponding Author
maxim.balakirev@cea.fr

■ REFERENCES

(1) Lavis, L. D.; Raines, R. T. *ACS Chem. Biol.* **2008**, *3*, 142.
(2) (a) Rosania, G. R.; Lee, J. W.; Ding, L.; Yoon, H. S.; Chang, Y. T. *J. Am. Chem. Soc.* **2003**, *125*, 1130. For a review, see: (b) Vendrell, M.; Lee, J. S.; Chang, Y. T. *Curr. Opin. Chem. Biol.* **2010**, *14*, 383.
(3) Simeonov, A.; Jadhav, A.; Thomas, C. J.; Wang, Y.; Huang, R.; Southall, N. T.; Shinn, P.; Smith, J.; Austin, C. P.; Auld, D. S.; Inglese, J. *J. Med. Chem.* **2008**, *51*, 2363.
(4) Mugherli, L.; Burchak, O. N.; Balakireva, L. A.; Thomas, A.; Chatelain, F.; Balakirev, M. Y. *Angew. Chem., Int. Ed.* **2009**, *48*, 7639.
(5) (a) Groebke, K.; Weber, L.; Mehlin, F. *Synlett* **1998**, 661. (b) Blackburn, C.; Guan, B.; Fleming, P.; Shiosaki, K.; Tsai, S. *Tetrahedron Lett.* **1998**, *39*, 3635. (c) Bienayme, H.; Bouzid, K. *Angew. Chem., Int. Ed.* **1998**, *37*, 2234. (d) Dömling, A. *Chem. Rev.* **2006**, *106*, 17. (e) Hulme, C.; Lee, Y.-S. *Mol. Diversity* **2008**, *12*, 1.
(6) (a) Hulme, C.; Bienayme, H.; Nixey, T.; Chenera, B.; Jones, W.; Tempest, P.; Smith, A. *Methods Enzymol.* **2003**, *369*, 469. (b) Lin, Q.; Blackwell, H. E. *Chem. Commun.* **2006**, 2884.
(7) (a) de Silva, A. P.; Gunaratne, H. Q. N.; Gunnlaugsson, T.; Huxley, A. J. M.; McCoy, C. P.; Rademacher, J. T.; Rice, T. E. *Chem. Rev.* **1997**, *97*, 1515. (b) Lakowicz, J. R. *Principles of Fluorescence Spectroscopy*, 2nd ed.; Kluwer Academic/Plenum Publishers: New York, 1999.
(8) Papadopoulos, V.; Baraldi, M.; Guilarte, T. R.; Knudsen, T. B.; Lacapère, J. J.; Lindemann, P.; Norenberg, M. D.; Nutt, D.; Weizman, A.; Zhang, M. R.; Gavish, M. *Trends Pharmacol. Sci.* **2006**, *27*, 402.
(9) Clayton, T.; Chen, J. L.; Ernst, M.; Richter, L.; Cromer, B. A.; Morton, C. J.; Ng, H.; Kaczorowski, C. C.; Helmstetter, F. J.; Furtmuller, R.; Ecker, G.; Parker, M. W.; Sieghart, W.; Cook, J. M. *Curr. Med. Chem.* **2007**, *14*, 2755.
(10) (a) Kozikowski, A. P.; Ma, D.; Brewer, J.; Sun, S.; Costa, E.; Romeo, E.; Guidotti, A. *J. Med. Chem.* **1993**, *36*, 2908. (b) Trapani, G.; Franco, M.; Ricciardi, L.; Latrofa, A.; Genchi, G.; Sanna, E.; Tuveri, F.; Cagetti, E.; Biggio, G.; Liso, G. *J. Med. Chem.* **1997**, *40*, 3109.
(11) (a) Pretner, E.; Amri, H.; Li, W.; Brown, R.; Lin, C. S.; Makariou, E.; Defeudis, F. V.; Drieu, K.; Papadopoulos, V. *Anticancer Res.* **2006**, *26*, 9. (b) Fafalios, A.; Akhavan, A.; Parwani, A. V.; Bies, R. R.; McHugh, K. J.; Pflug, B. R. *Clin. Cancer Res.* **2009**, *15*, 6177.